Computers, Materials & Continua

Tech Science Press

https://doi.org/10.32604/cmc.2026.082720

ARTICLE

An Explainable Hybrid Opt-GRU-KAN Architecture for Lithium-Ion Battery Health Prediction

Riya Sharma[1,*], Ashima Singh[1], Anju Bala[1] and Mukesh Singh[2]

[1]Computer Science and Engineering Department, Thapar Institute of Engineering and Technology, Patiala, India
[2]Electrical and Instrumentation Engineering Department, Thapar Institute of Engineering and Technology, Patiala, India

*Corresponding Author: Riya Sharma. Email: rsharma_phd22@thapar.edu

Received: 30 March 2026; Accepted: 08 May 2026; Published: 23 July 2026

ABSTRACT: State of health (SoH) prediction of lithium-ion batteries is a critical yet challenging task due to the complex, highly non-linear, and time-dependent nature of degradation processes under diverse operating conditions. Variability in usage patterns, environmental factors, and electrochemical dynamics further limits the robustness and generalisation capability of conventional estimation models. This study proposes a hybrid deep learning framework that combines Gated Recurrent Units (GRUs) with Kolmogorov–Arnold Networks (KANs) to address these challenges. GRUs are employed to effectively capture temporal dependencies in sequential battery data, while KANs enhance the model's ability to learn complex non-linear functional relationships. To improve model transparency and mitigate the black-box nature of deep learning approaches, Explainable Artificial Intelligence (XAI) techniques are integrated to provide interpretable insights into prediction outcomes. Additionally, Optuna-based hyperparameter optimisation is utilised to systematically identify optimal model configurations for enhanced predictive performance. The proposed model is trained using the Toyota Research Institute dataset and validated on real-time electric vehicle battery data collected at Thapar Institute of Engineering and Technology, along with the benchmark CALCE dataset, ensuring robustness across multiple data distributions. Experimental results demonstrate that the hybrid GRU–KAN framework outperforms existing state-of-the-art approaches in terms of accuracy and generalisation. Quantitative evaluation using RMSE, MSE, and MAE shows prediction errors within 1%, indicating high precision in SoH estimation. Module ablation studies further confirm the contribution of each component to the overall model performance.

KEYWORDS: Battery management system; electric vehicle; gated recurrent unit; Kolmogorov Arnold network; lithium-ion battery; optuna optimiser; state of health

1 Introduction

The rising demand for electric vehicles (EVs) is primarily driven by significant technological advancements. With growing environmental awareness, more people are opting for eco-friendly transportation alternatives [1]. A critical factor in this shift is the efficiency of battery-operated vehicles, which convert most electrical energy directly into wheel power [2]. Central to the performance of these vehicles is the battery, with lithium-ion batteries being the most widely used due to their rechargeable nature and portability [3]. However, the consistent recharging of these batteries inevitably leads to ageing, resulting in a decline in their energy storage capacity. This ageing process reduces reliability, power output, and the ability to hold a charge [4]. Monitoring critical parameters is essential to ensure the efficient use of Li-ion batteries, with the State of Health (SoH) being the most important. SoH is a key metric for assessing battery performance, as it provides crucial insights into capacity degradation and ensures safe driving conditions [5]. Accurately estimating SoH, however, is challenging due to the gradual nature of battery degradation [6]. As the number of charge cycles increases, data-driven methods outperform model-based approaches in predicting SoH over extended battery lifespans. Conversely, while model-based methods may initially provide accurate predictions, they often need help maintaining precision over numerous cycles due to the complexities and non-linearities involved.

Moreover, machine learning emerged as a powerful tool for developing accurate and reliable prediction models. Vakharia et al. [7] introduced a novel approach to estimating the discharge capacity of lithium-ion batteries by combining optimised XAI with stacked long short-term memory (LSTM) models and utilising the jellyfish optimisation algorithm to enhance prediction accuracy. In contrast to the findings of [7], Jafari and Byun [8] presented an innovative method for estimating the Remaining Useful Life (RUL) of lithium-ion batteries in electric vehicles. This approach integrates measurable features, such as discharge time and temperature, with advanced machine learning techniques, emphasising the role of XAI in ensuring model transparency and trustworthiness. Moreover, Zhang et al. [9] provided additional insights by showing an improved transformer model optimised with a Stacked Denoising Autoencoder (SDAE) for predicting the RUL of lithium-ion batteries under varying charging and discharging conditions. This model leverages diverse NASA datasets, integrating multiple health factors and employing Principal Component Analysis (PCA) for data fusion to enhance prediction accuracy [10].

Although Wang et al. [11] emphasised on a hybrid model combining Empirical Mode Decomposition (EMD), Variance Contribution Ratio (VCR), GRU, and RF to estimate battery SoH. The estimation method uses a combination of machine and deep learning models. The model has not been validated for different battery chemistries. In a related study, Zhao and Behdad [12] proposed a framework for estimating electric vehicle batteries' SoH using transformer-based neural networks. The research highlights the necessity of comprehensive datasets to capture real-world variability in battery usage and suggests future research directions to enhance model robustness and adaptability. An extension of this idea can be found in Gu et al. [13] where a novel method for SoH estimation of lithium-ion batteries using a convolutional neural network (CNN)-Transformer framework, emphasising the importance of data preprocessing techniques, such as the Pearson correlation coefficient (PCC) and PCA, to improve model efficiency, has been presented.

Moreover, Chen et al. [14] developed a new algorithm for SoH estimation of lithium-ion batteries using a regression vision transformer (RVIT) network. Based on the transformer model, this network effectively captures the temporal and spatial information embedded in battery data and has been trained and tested on NASA and CACLE datasets. Similarly, Jia et al. [15] proposed a hybrid model that integrates a bidirectional gated recurrent unit with a transformer utilising a multi-head attention mechanism. This model extracts time series features from indirect health indicators (HI), demonstrating improved accuracy, robustness, and generalisation, as evidenced by experiments on NASA's PCoE lithium-ion battery data.

Additionally, Wang et al. [16] introduced method for lithium-ion battery SOH estimation using an Enhanced Whale Optimization Algorithm for feature selection and Support Vector Regression (SVR). Key features are selected from charge data, with improved accuracy through dynamic thresholding and random forest-based weighting. The method faces limitations in generalisation and lacks comparison with advanced deep learning models. Moreover, Dong et al. [17] proposed a robust RUL prediction framework for lithium-ion batteries using a CNN-LSSVR model optimised by mutation particle swarm optimisation. It introduces discharge energy as a novel RUL indicator and leverages Multi-Resolution Singular Value Decomposition (MRSVD) for effective noise reduction. The approach addresses small-sample and high-noise challenges in battery prognostics.

Furthermore, Yao et al. [18] introduced a mechanism-empowered feature engineering approach for accurate Li-ion battery SoH estimation. It integrates mechanistic signal analyses—IC, DV, QV, and a novel

ICD method—with statistical techniques like PCC, GRA, and MRMR to extract robust and interpretable features. The model relies on controlled datasets and handcrafted features, limiting adaptability to real-world conditions and diverse battery chemistries. Lastly, Lu et al. [19] proposed an estimation method based on a deep learning neural network with fine-tuned transfer learning. This approach addresses the limitations of conventional machine learning models that assume identical data distributions across training and testing sets.

The examined literature shows considerable advances in battery health estimation utilising machine learning, particularly transformer-based designs. However, critical research gaps given in Table 1 remain: limited exploration of model generalisation across diverse battery chemistries and operational conditions, inadequate integration of real-world variability in datasets, particularly regarding long-term ageing effects, lack of standardisation in preprocessing techniques leading to inconsistent performance across studies, and limited focus on enhancing the transparency of deep learning models beyond basic explainability. This encourages additional research into developing robust, interpretable models that can generalise across multiple battery types and environmental circumstances while utilising standardised data fusion and preprocessing methodologies to increase accuracy and consistency in health and longevity forecasts.

Table 1: Existing literature and their methodologies applied for SoH estimation.

Authors [Ref]	Dataset	Estimation Method	Parameter Tuning	XAI	Real-Time Data	Ablation Analysis
Vakharia et al. [7]	NASA	Stacked LSTM with Optimised Ex-AI	✓	✓	✗	✗
Jafari and Byun [8]	NASA	Feature based ML approach	✓	✓	✗	✗
Zhang et al. [9]	NASA	SDAE-Transformer	✗	✗	✗	✗
Wang et al. [11]	NASA	EMD-VCR-GRU-RF	✗	✗	✗	✓
Zhao and Behdad [12]	NASA	Transformer	✓	✗	✗	✗
Gu et al. [13]	NASA	CNN-Transformer	✗	✗	✗	✗
Chen et al. [14]	NASA, CALCE	Vision-Transformer	✗	✗	✗	✗
Jia et al. [15]	NASA	BiGRU-Transformer	✗	✗	✗	✗
Wang et al. [16]	NASA	SVR	✓	✗	✗	✗
Dong et al. [17]	NASA, Toyota	CNN-LSSVR	✓	✗	✗	✓
Yao et al. [18]	NASA, CALCE, Toyota	MRMR-ML approach	✓	✗	✗	✗
Lu et al. [19]	NASA, CALCE, Oxford	DNN-Transfer Learning	✗	✗	✗	✗

(Continued)

Table 1 (continued)

Authors [Ref]	Dataset	Estimation Method	Parameter Tuning	XAI	Real-Time Data	Ablation Analysis
Optuna GRU-KAN with XAI	Toyota, CALCE, Real-Time	GRU-KAN model	✓	✓	✓	✓

Contributions and Structure of the Paper

The main contributions of this study can be summarised as follows:

- Integrating the GRU-KAN hybrid architecture for SoH estimation effectively addresses the constraints of previous methodologies, considerably enhancing prediction accuracy while minimising reliance on large training datasets when compared to traditional neural network techniques.
- The embedded XAI framework overcomes the interpretability challenges in battery health estimation, providing actionable insights into degradation mechanisms that enable proactive maintenance strategies and targeted interventions before a critical failure occurs.
- The Optuna-based hyperparameter optimisation framework demonstrates superior adaptability and efficient model training across diverse operating conditions, proving the model's performance remains robust regardless of variations between training and target battery characteristics.
- Module ablation analysis confirming the hybrid model's superior accuracy and generalisation capabilities in capturing both non-linear degradation patterns and temporal dependencies critical for reliable state of health predictions.

The subsequent sections are structured as follows: Section 2 explains the proposed methodology. Sections 3 and 4 present results. Section 5 provides comparative analysis. Section 6 concludes.

2 Model Development

2.1 Experimental Data and Setup

The Toyota Research Institute dataset has been chosen to train selected algorithms. Real-time data and CALCE data [20] have been utilised to validate the proposed model given in Table 2. The minimum hardware requirement to implement the work is Windows 11 with an Intel i5-1135G7 CPU and 8 GB RAM. Jupyter Notebook with Python 3.9 has been used to train and test the proposed model.

Table 2: Dataset-specific test conditions.

Dataset	Chemistry	Voltage (V)	Capacity (Ah)
Toyota	LFP	3.3	1.1
CALCE	$LiCoO_2$	2.0	1.1
Real-time	NMC	3.7	2.0

2.1.1 Toyota Data

The dataset comprises 124 commercial LFP cells manufactured by A123 Systems, cycled under different charge-discharge conditions. The cells have a nominal voltage of 3.3 V and a capacity of 1.1 Ah and have been cycled in a temperature chamber of 30°C. End of life was defined as several cycles till 80% of the nominal capacity and results from 124 batteries with cycle life from 150 to 2300, and 72 fast charging conditions were gathered. According to the manufacturer's suggested fast charging rate, charging rates were from 3.6 C to extreme fast-charging (XFC) settings of 6 C. A total of 10 batteries have been selected for testing, namely b1c0, b1c1, b2c0, b2c1, b3c0, b3c1, b1c3, b2c3, b3c3, and b1c5. The batteries were chosen so that some have degradation from 0–500 cycles; some have 500–1000, and others have 1000–1500 and above 2000 cycles to have variability in the data.

2.1.2 CALCE Data

The CALCE battery dataset consists of two CS2 batteries: CS2_36 and CS2_37. The charging of the batteries was done at a constant current (CC) mode at a 1C rate until the voltage reached 4.2 V. Further, the batteries have been charged at constant voltage (CV) mode at 4.2 V until the current dropped below 0.05 A [21].

2.1.3 Real-Time Data

Real-time data was acquired from an NMC battery deployed in the E-Scooter at Thapar Institute, India. The complete battery pack comprises 14 series-connected cells with a nominal voltage of 51.8 V and 28 Ah capacity (3.7 V, 2.0 Ah per cell), charged in CC-CV mode. The data has been fetched through an IoT module in the BMS and a cloud interface at 3-s intervals across 30 measured parameters, providing cell-level insight into degradation behaviour under variable operational loads [20,22].

2.2 Proposed Model

In this paper, a hybrid GRU-KAN model with Optuna has been proposed, for which the methodology is shown in Fig. 1. The model consists of four parts: data pre-processing, GRU and KAN model building, Optuna hyperparameter optimisation, and model explainability. Module ablation analysis has been done to find the contribution of each model for SoH estimation.

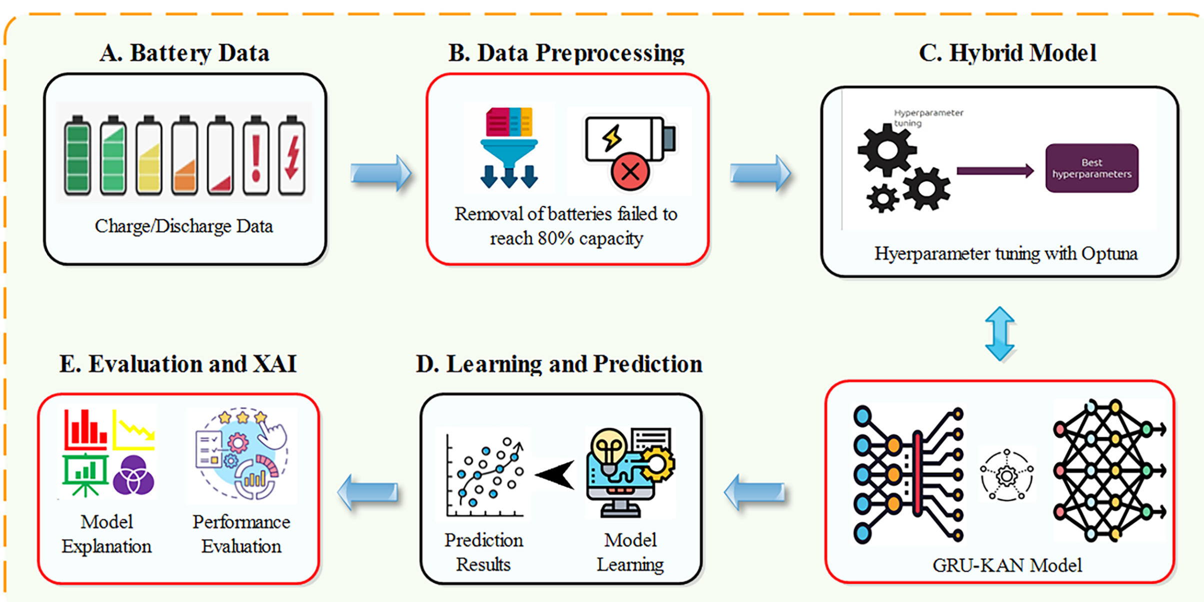

Figure 1: Flow chart of the proposed model.

2.2.1 Data Pre-Processing

The battery cycling data had three batches, and it was necessary to preprocess it to obtain quality data and organise it properly. The detailed pre-processing has been given in Algorithm 1. Among batch 1, five cells declared to have failed to reach 80% capacity, namely b1c8, b1c10, b1c12, b1c13, and b1c22, were excluded from further consideration. All measurements were merged with batch1 (b1c0–b1c4) cells in batch2 (b2c7, b2c8, b2c9, b2c15, b2c16), resulting in an extension of 662, 981, 1060, 208, and 482 cycles in cycle life, respectively. Six cells (b3c37, b3c2, b3c23, b3c32, b3c42, b3c43) were removed from batch 3 due to noisy measurements. The dataset was partitioned into a train set (odd-indexed cells, batches 1–2), a primary test set (even-indexed cells and battery 83), and a secondary test set (remaining batch 3 cells). The discharge capacity (Qd) was monitored in each battery cycle, deteriorating to end-of-life at 0.8 Ah (80% nominal capacity).

Algorithm 1: Battery capacity analysis

Require: Battery data batches B_1, B_2, B_3
Ensure: Clean dataset and analysis splits
Remove invalid batteries from B_1, B_2, B_3
Merge overlapping batteries between B_1 and B_2
$bat\_dict \leftarrow B_1 \cup B_2 \cup B_3$
$N \leftarrow |bat\_dict|$
$test\_ind \leftarrow \{i : i \text{ is even}, i < N\} \cup \{83\}$
$train\_ind \leftarrow \{i : i \text{ is odd}, i < N\}$
for all battery $b \in bat\_dict$ **do**
    Plot discharge capacity vs. cycle number
end for
Add threshold line at 80% capacity

2.2.2 GRU-KAN Model

The algorithm of the proposed model is given in Algorithm 2, and the layered architecture has been shown in Fig. 2. The GRU model adapts the recurrent neural network that intends to resolve the vanishing gradient problem. GRU has a gating mechanism with fewer parameters than LSTM and can deal with long-term sequences capturing time-series data. GRU incorporates two gates: the update gate and the reset gate [23]:

$$z_t = \sigma(W_z \cdot [h_{t-1}, x_t] + b_z), \qquad r_t = \sigma(W_r \cdot [h_{t-1}, x_t] + b_r) \tag{1}$$

where z_t and r_t represent update and reset gates, σ is the sigmoid function, W_z, W_r are weight matrices, and b_z, b_r are biases.

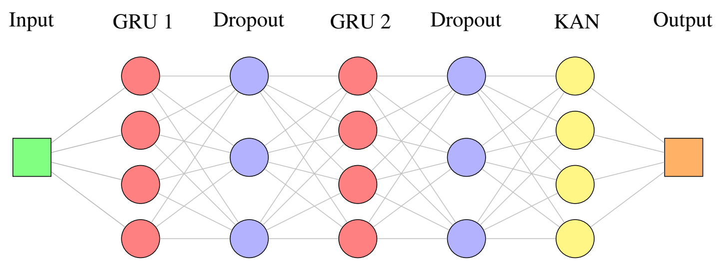

Figure 2: Node-level architecture of the proposed GRU-KAN model.

Algorithm 2: Hybrid GRU-KAN battery capacity prediction with SHAP analysis

Require: Battery dataset $\mathcal{B} = \{(c_i, q_i)\}_{i=1}^{N}$, sequence length τ, trials K
Ensure: Optimised model $\mathcal{M}^*$ with interpretability

1: $Q \leftarrow \text{MinMaxScaler}(q_{1:N})$; create sequences X_t; split 70/15/15
2: $h_t^1 = \text{GRU}_1(X_t)$; $d_1 = \text{Dropout}(h_t^1)$
3: $h_t^2 = \text{GRU}_2(d_1)$; $d_2 = \text{Dropout}(h_t^2)$
4: $k_t = \sin(W_k d_2 + b_k) \cdot \cos(W_k d_2 + b_k)$; $\hat{y}_t = \text{Dense}(k_t)$
5: **for** $i = 1$ to K **do**
6: Sample $\theta_i \sim \Theta$; $\mathcal{L}_i \leftarrow \text{MSE}(\mathcal{M}(\theta_i, \mathcal{D}_{val}))$
7: **if** $\mathcal{L}_i > \text{median}(\mathcal{L}_{1:i-1})$ **then**
8: Prune trial
9: **end if**
10: **end for**
11: $\theta^* \leftarrow \arg\min \mathcal{L}_i$
12: $\phi \leftarrow \text{KernelSHAP}(\mathcal{M}^*, \mathcal{D}_{train})$; generate importance plots **return** $\mathcal{M}^*, \theta^*, \phi$

KAN models are an application of the Kolmogorov-Arnold representation theorem. Unlike MLPs, KAN has learnable activation functions between neurons [24,25]. For any continuous function f:

$$f(x_1, \ldots, x_n) = \sum_{i=1}^{2n+1} \psi_i\left(\sum_{j=1}^{n} \phi_{ij}(x_j)\right) \tag{2}$$

where ϕ_{ij} and ψ_i are inner and outer transformation functions learnt via B-splines. Applied to battery input $x = [V, I, T, IR, \text{Cycle}]$, KAN decomposes the SoH relationship as:

$$h_i = \sum_{j=1}^{d} \phi_{ij}(x_j), \qquad SoH = \sum_{i=0}^{2d} \Phi_i(h_i) \tag{3}$$

The GRU hidden state integrates temporal patterns via the update gate z_t (long-term degradation) and reset gate r_t (selective forgetting after rest periods). The SoH prediction layer is:

$$\hat{y}_{SoH} = W_{SoH} h_t + b_{SoH} \tag{4}$$

2.2.3 Optuna Optimiser

Optuna dynamically constructs the hyperparameter search space and minimises a validation objective using Bayesian optimisation, tree-structured Parzen estimators, and pruning of unpromising trials [26]:

$$\theta^* = \arg\min_{\theta \in \Theta} f(\theta) \tag{5}$$

where θ is the hyperparameter vector, Θ the search space, and $f(\theta)$ the validation loss.

2.2.4 Explainability

XAI bridges the gap between predictive accuracy and model transparency in DL-based SoH estimation [27]. SHAP, a game-theory-based post-hoc method, assigns each feature a contribution score by evaluating all feature coalitions [28]. Kernel SHAP provides an efficient approximation:

$$g(z') = \phi_0 + \sum_{j=1}^{M} \phi_j z'_j \tag{6}$$

where g is the explanation model, $z' \in \{0,1\}^M$ is the coalition vector, and ϕ_j is the Shapley value for feature j.

2.3 Module Ablation Analysis

Each core module (GRU, KAN, Optuna) was removed or replaced in isolation to quantify its contribution [29]. Replacing GRU with Conv-GRU degraded temporal tracking; removing KAN reduced non-linear modelling capacity; omitting Optuna lowered prediction accuracy. RMSE, MSE, and R^2 results confirm all three components are necessary for optimal performance.

2.4 Evaluation Metrics

Performance is evaluated using RMSE, MSE, MAE, MAPE, and R^2:

$$RMSE = \sqrt{\frac{\sum (SoH_{true} - SoH_{pred})^2}{n}}, \quad MSE = \frac{\sum (SoH_{true} - SoH_{pred})^2}{n} \tag{7}$$

$$MAE = \frac{\sum |SoH_{true} - SoH_{pred}|}{n}, \quad R^2 = 1 - \frac{\sum (SoH_{true} - SoH_{pred})^2}{\sum (SoH_{true} - SoH_{mean})^2} \tag{8}$$

3 Results and Performance Evaluation

Eight architectures were evaluated on battery cycling data up to 2000 cycles; full quantitative results are in Table 3. Figs. 3 and 4 show the baseline and proposed model prediction results, respectively.

Table 3: Error metrics for different models.

Models	RMSE (%)	MSE	MAE (%)	R^2 (%)
KAN	4.05	0.16	3.97	29.53
GRU	0.63	0.0037	0.23	97.77
Conv-GRU	2.75	0.08	2.67	58.06
Optuna KAN	2.37	0.06	1.44	68.83
Optuna GRU	1.67	0.027	1.56	84.53
Optuna Conv-GRU	2.53	0.064	2.35	64.48
Optuna LSTM	0.62	0.0039	0.17	97.79
Optuna KAN-GRU (Proposed)	0.57	0.0033	0.11	98.56

The Conv-GRU (Fig. 3a) shows moderate accuracy but fails to track degradation between cycles 500–1000. The standard GRU (Fig. 3b) tracks capacity changes more precisely, though it remains unreliable at high cycle counts. Standalone KAN (Fig. 3c) exhibits the weakest baseline performance with systematic overestimation early in cycling, confirming that temporal modelling elements are essential. The Optuna GRU (Fig. 3d) achieves strong alignment but shows minor underprediction outliers in the 1.06–1.07 Ah range.

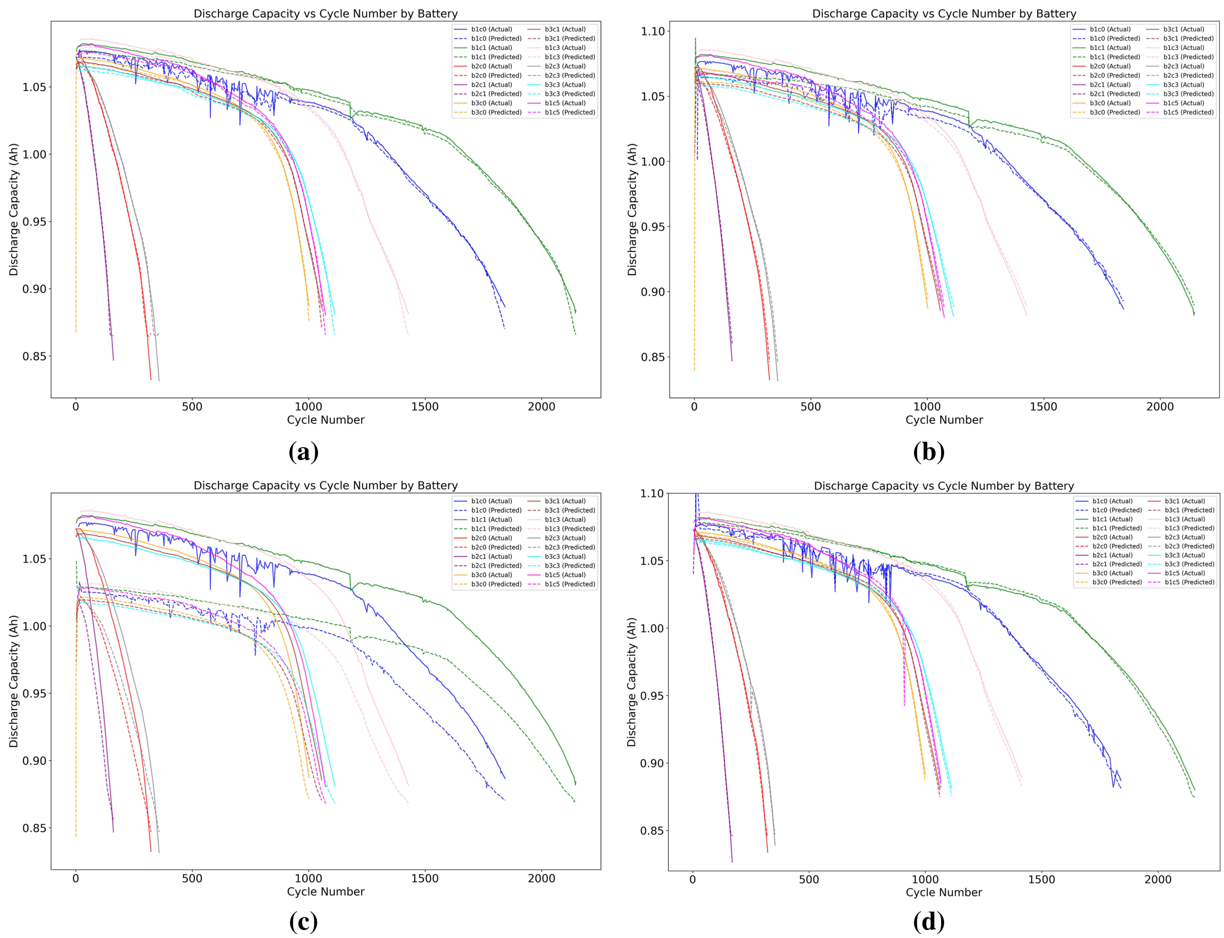

Figure 3: SoH estimation results for baseline models (**a**) Conv-GRU (**b**) GRU (**c**) KAN (**d**) Optuna GRU.

The proposed Optuna GRU-KAN (Fig. 4) maintains consistent accuracy from cycle 1 to 2000, accurately capturing gradual fade, rapid knee-point transitions, and temporary capacity recovery at cycles 1000–1500—a direct result of integrating GRU's temporal memory with KAN's non-linear function modelling. The model also demonstrates robustness to cell-to-cell variability, a critical requirement for practical BMS deployment.

Explainability Results

The SHAP analysis (Fig. 5) provides local and global explanations. Locally (Fig. 5a), for Sample 42, internal resistance, cycle number, and minimum temperature positively influence the prediction, while average temperature and charge capacity reduce it, yielding f(X) = 0.385 against baseline E[f(X)] = 0.371. Globally (Fig. 5b), charge capacity, cycle number, and internal resistance are the dominant SoH features; Tavg, Tmin, and QD show minimal impact, guiding feature selection and model refinement.

4 Correlation Analysis

Figs. 6 and 7 show correlation plots between actual and predicted discharge capacity. Conv-GRU (Fig. 6a) shows moderate alignment with noticeable scatter at both capacity extremes. GRU (Fig. 6b) improves alignment but remains inconsistent above 1.05 Ah. Standalone KAN (Fig. 6c) shows the weakest correlation with systematic underprediction above 1.025 Ah. Optuna GRU (Fig. 6d) achieves a strong linear relationship across the full range with only small outlier clusters near 1.06–1.07 Ah.

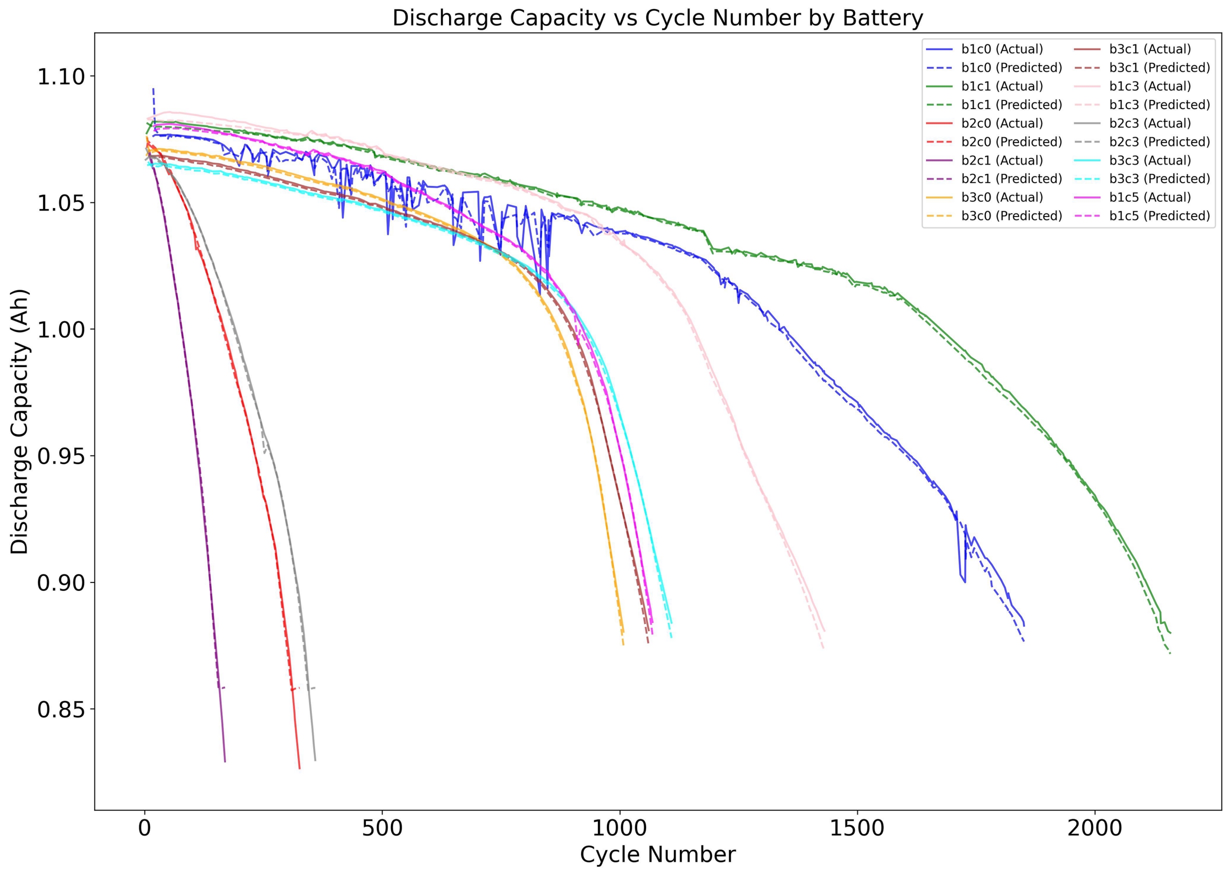

Figure 4: SoH estimation results for proposed Optuna GRU-KAN.

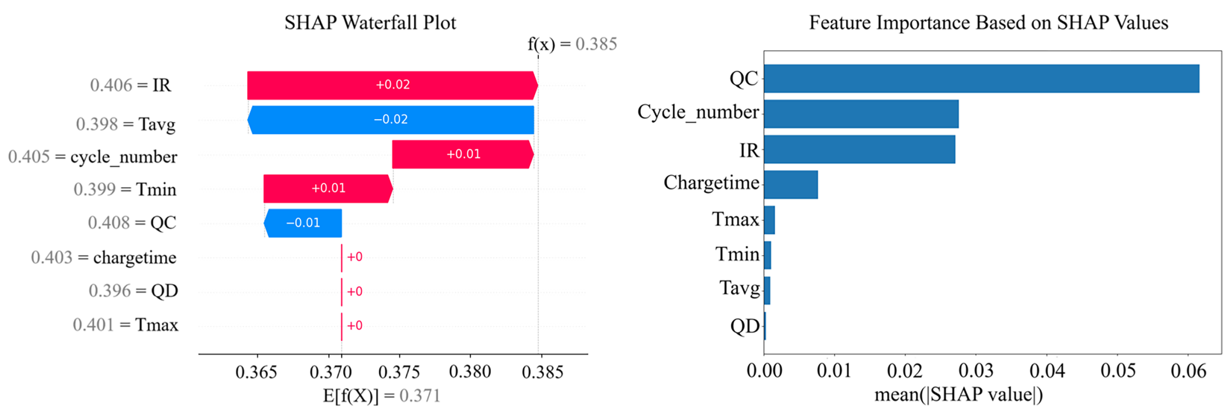

(a) **(b)**

Figure 5: Explainability results (**a**) local SHAP waterfall for sample 42 (**b**) global feature importance.

The proposed Optuna GRU-KAN (Fig. 7) achieves the tightest alignment across the full 0.875–1.075 Ah range with minimal outliers at all capacity levels, confirming its superiority. Across all evaluated models, correlation strength followed as KAN worst, followed by Conv-GRU variants, with the proposed hybrid consistently best.

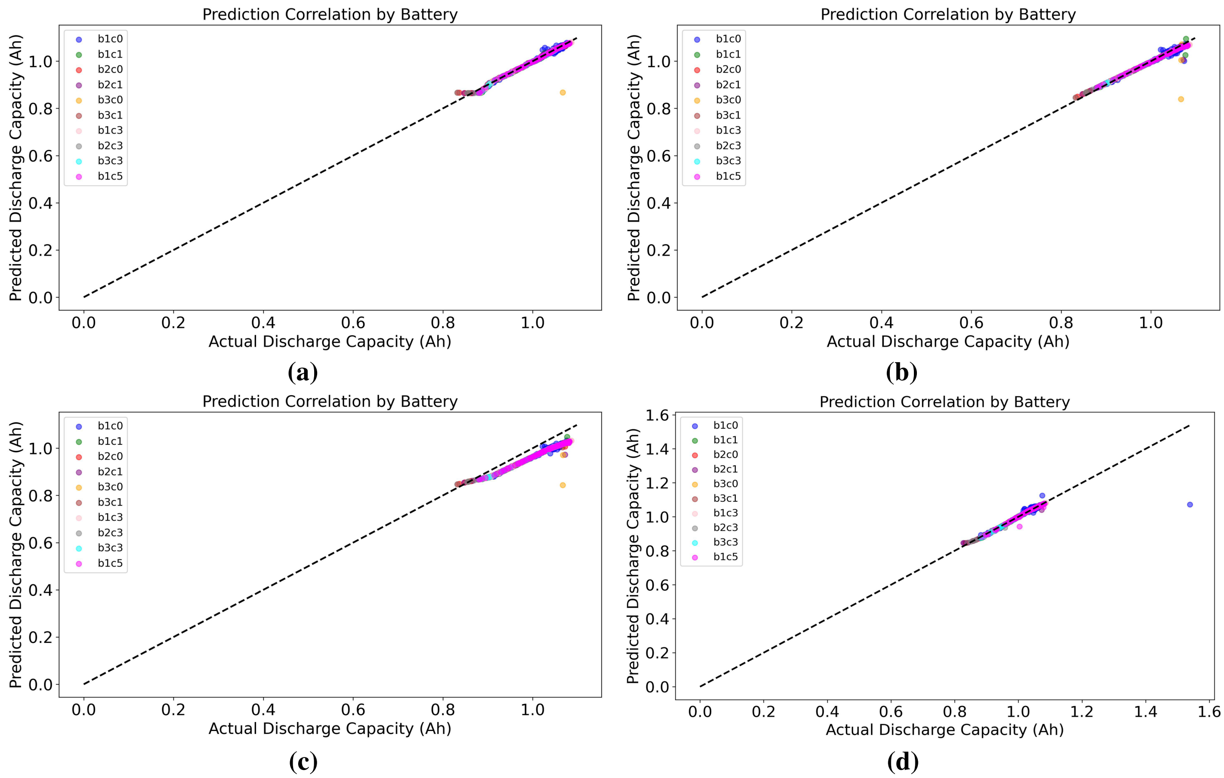

Figure 6: Prediction correlation plots for baseline models (**a**) Conv-GRU (**b**) GRU (**c**) KAN (**d**) Optuna GRU.

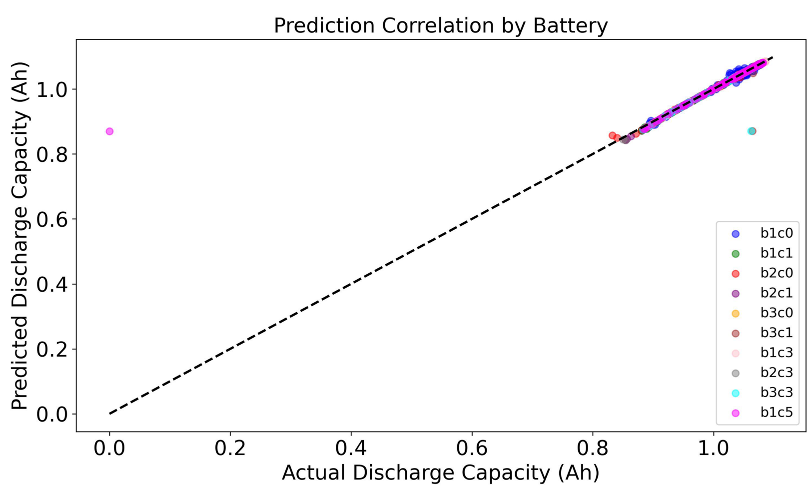

Figure 7: Prediction correlation plot for proposed Optuna GRU-KAN.

5 Comparative Analysis

Table 3 and Fig. 8 present the full ablation results. Baseline KAN performed poorly (RMSE: 4.05%, R^2: 29.53%); Conv-GRU was moderate (RMSE: 2.75%); GRU was the strongest baseline (RMSE: 0.63%, R^2: 97.77%). Optuna LSTM closely matched GRU (RMSE: 0.62%). The proposed Optuna GRU-KAN surpassed all models on every metric (RMSE: 0.57%, MAE: 0.11%, R^2: 98.56%). Table 4 and Fig. 9 confirm Optuna GRU-KAN (RMSE: 0.0020, MAE: 0.00040) substantially outperforms prior CNN-LSSVR, MRSVD-CNN-LSSVR, and MRMR-GPR4 methods.

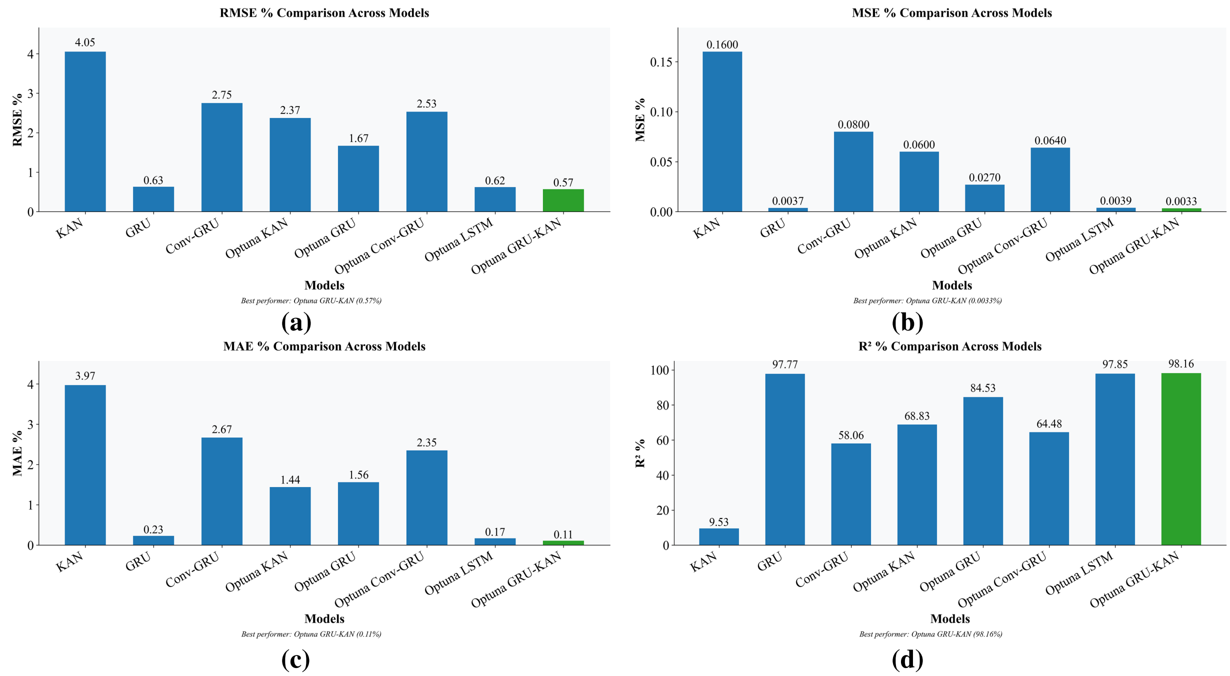

Figure 8: Model evaluation plots (**a**) RMSE (**b**) MSE (**c**) MAE (**d**) R^2.

Table 4: Comparison with previous work.

Models	RMSE	MAE
CNN-LSSVR [17]	0.0131	0.1372
MRSVD-CNN-LSSVR [17]	0.0161	0.01376
MRMR-GPR4 [18]	0.0126	0.00405
Optuna GRU-KAN	0.0020	0.00040

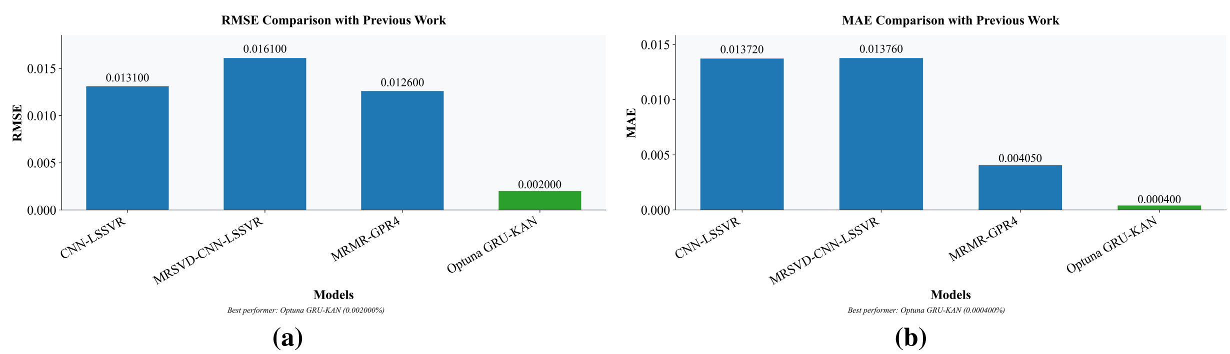

Figure 9: Error comparison with previous work: (**a**) RMSE (**b**) MAE.

Validation of the Proposed Model

The model was validated on real-time EV battery data (Fig. 10), achieving RMSE of 0.49 and MSE of 0.0024, confirming robust generalisation to variable loads and environmental conditions. Validation on CALCE data (Fig. 11, Table 5) yielded RMSE below 0.010 for both CS2 batteries, further demonstrating cross-chemistry robustness.

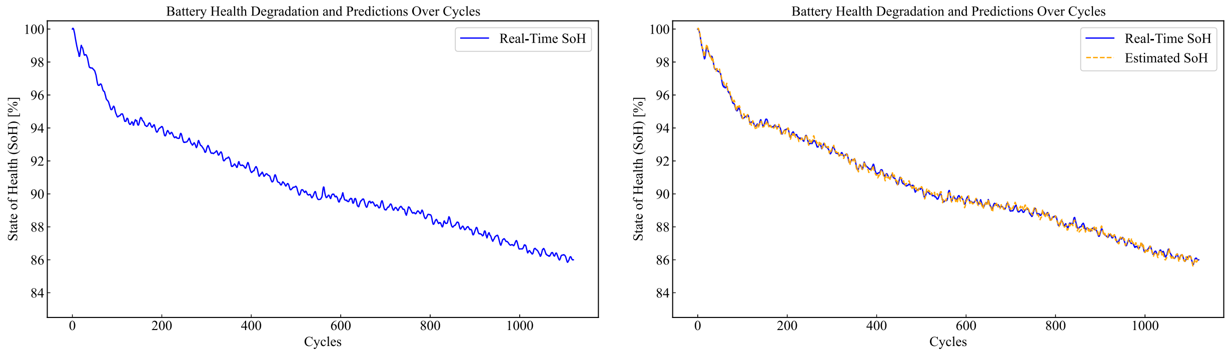

(a) **(b)**

Figure 10: SoH prediction for real-time data (**a**) real-time data plot (**b**) prediction plot.

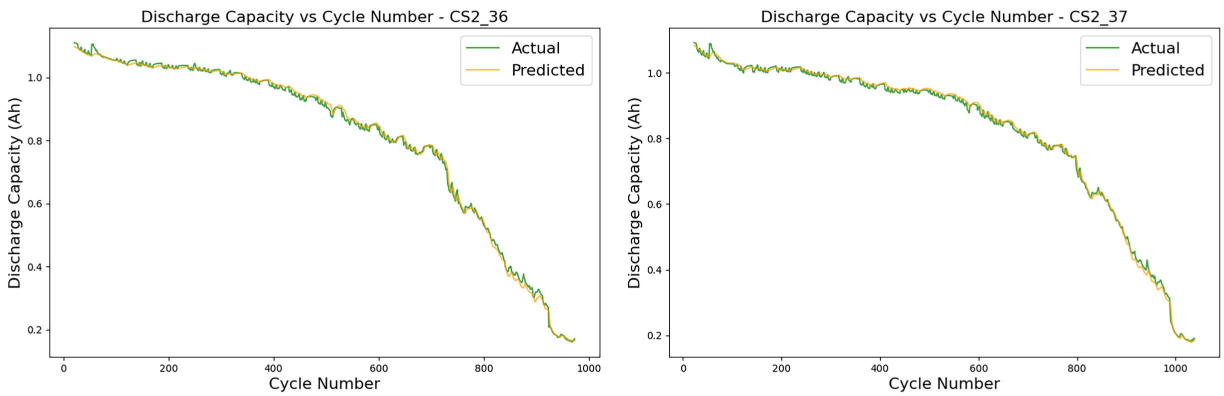

(a) **(b)**

Figure 11: Discharge capacity prediction for CALCE data (**a**) CS2_36 (**b**) CS2_37.

Table 5: Error metrics for CALCE data.

Battery	RMSE	MSE	MAE
CS2_35	0.010	0.0001	0.008
CS2_36	0.009	0.00009	0.007

6 Conclusion

This paper presents a hybrid GRU-KAN framework optimised by Optuna for lithium-ion battery SoH estimation. The proposed architecture achieves superior results on all metrics (RMSE: 0.57%, MSE: 0.0033, MAE: 0.11%, R^2: 98.56%), outperforming all baseline and optimised variants. Module ablation confirmed each component's necessity. Validation across Toyota training data, real-time EV data, and the CALCE benchmark demonstrates strong generalisation across chemistries and operating conditions. The integrated SHAP-based XAI framework provides transparent, actionable insights into degradation mechanisms, offering significant potential for real-world deployment in intelligent battery management systems.

Acknowledgement: None.

Funding Statement: The authors gratefully acknowledge the Ministry of Electronics and Information Technology (MeitY), Government of India, Project Identification No. 25(2)/2021-ESDA.

Author Contributions: Conceptualization: Riya Sharma, Ashima Singh; methodology: Riya Sharma; validation: Riya Sharma, Ashima Singh, Mukesh Singh; formal analysis: Riya Sharma, Anju Bala; data curation: Anju Bala; writing—original draft: Riya Sharma, Ashima Singh; writing—review and editing: Mukesh Singh, Ashima Singh, Riya Sharma; supervision and project administration: Ashima Singh; funding acquisition: Mukesh Singh. All authors reviewed and approved the final version of the manuscript.

Availability of Data and Materials: Available from the corresponding author upon reasonable request.

Ethics Approval: Not applicable.

Conflicts of Interest: The authors declare no competing interests.

References

1. Guo N, Zhang X, Zou Y, Lenzo B, Zhang T. A computationally efficient path-following control strategy of autonomous electric vehicles with yaw motion stabilization. IEEE Trans Transp Electrif. 2020;6(2):728–39. doi:10.1109/tte.2020.2993862.
2. Islam R, Rafin SMSH, Mohammed OA. Comprehensive review of power electronic converters in electric vehicle applications. Forecasting. 2023;5(1):22–80. doi:10.3390/forecast5010002.
3. Kulova TL, Fateev VN, Seregina EA, Grigoriev AS. A brief review of post-lithium-ion batteries. Int J Electrochem Sci. 2020;15(8):7242–59. doi:10.20964/2020.08.22.
4. Ramkumar MS, Reddy CSR, Ramakrishnan A, Raja K, Pushpa S, Jose S, et al. Review on Li-ion battery with battery management system in electrical vehicle. Adv Mater Sci Eng. 2022;2022(3):3379574. doi:10.1155/2022/3379574.
5. Kassim MRM, Jamil WAW, Sabri RM. State-of-charge (SOC) and state-of-health (SOH) estimation methods in battery management systems for electric vehicles. In: Proceedings of the 2021 IEEE International Conference on Computing (ICOCO); 2021 Nov 17–19; Kuala Lumpur, Malaysia. p. 91–6.
6. Vidal C, Malysz P, Kollmeyer P, Emadi A. Machine learning applied to electrified vehicle battery state of charge and state of health estimation: state-of-the-art. IEEE Access. 2020;8:52796–814. doi:10.1109/access.2020.2980961.
7. Vakharia V, Shah M, Nair P, Borade H, Sahlot P, Wankhede V. Estimation of lithium-ion battery discharge capacity by integrating optimized explainable-AI and stacked LSTM model. Batteries. 2023;9(2):125. doi:10.3390/batteries9020125.
8. Jafari S, Byun YC. Accurate remaining useful life estimation of lithium-ion batteries in electric vehicles based on a measurable feature-based approach with explainable AI. J Supercomput. 2024;80(4):4707–32. doi:10.1007/s11227-023-05648-8.
9. Zhang W, Jia J, Pang X, Wen J, Shi Y, Zeng J. An improved transformer model for remaining useful life prediction of lithium-ion batteries under random charging and discharging. Electronics. 2024;13(8):1423. doi:10.3390/electronics13081423.
10. Kamboj RK, Singh M, Singh A, Bala A. Explainable parallel GRU–LSTM model for predictive maintenance of lithium-ion batteries. Ionics. 2026;32(4):4227–43. doi:10.1007/s11581-026-07053-6.
11. Wang X, Hu B, Su X, Xu L, Zhu D. State of health estimation for lithium-ion batteries using random forest and gated recurrent unit. J Energy Storage. 2024;76:109796.
12. Zhao Y, Behdad S. State of health estimation of electric vehicle batteries using transformer-based neural network. J Energy Resour Technol. 2024;146(10):101703. doi:10.1115/1.4065762.
13. Gu X, See KW, Li P, Shan K, Wang Y, Zhao L, et al. A novel state-of-health estimation for the lithium-ion battery using a convolutional neural network and transformer model. Energy. 2023;262:125501. doi:10.1016/j.energy.2022.125501.

14. Chen L, Xie S, Lopes AM, Bao X. A vision transformer-based deep neural network for state of health estimation of lithium-ion batteries. Int J Electr Power Energy Syst. 2023;152:109233. doi:10.1016/j.ijepes.2023.109233.
15. Jia C, Tian Y, Shi Y, Jia J, Wen J, Zeng J. State of health prediction of lithium-ion batteries based on bidirectional gated recurrent unit and transformer. Energy. 2023;285(2):129401. doi:10.1016/j.energy.2023.129401.
16. Wang R, Xu X, Zhou Q, Zhang J, Wang J, Ye J, et al. State of health estimation for lithium-ion batteries using enhanced whale optimization algorithm for feature selection and support vector regression model. Processes. 2025;13(1):158. doi:10.3390/pr13010158.
17. Dong T, Sun Y, Liu J, Gao Q, Zhao C, Cao W. Remaining useful life prediction of lithium-ion batteries based on data preprocessing and CNN-LSSVR algorithm. Int J Electr Power Energy Syst. 2025;167:110619. doi:10.2139/ssrn.4952190.
18. Yao L, Wen J, Xiao Y, Zhang C, Shen Y, Cui G, et al. State of health estimation approach for li-ion batteries based on mechanism feature empowerment. J Energy Storage. 2024;84:110965. doi:10.1016/j.est.2024.110965.
19. Lu Z, Fei Z, Wang B, Yang F. A feature fusion-based convolutional neural network for battery state-of-health estimation with mining of partial voltage curve. Energy. 2024;288(2):129690. doi:10.1016/j.energy.2023.129690.
20. Singh A, Singh S, Kamboj RK, Bala A. Explainable OptiCNN-SLSTM hybrid model for enhanced lithium-ion battery state of health prediction. Sci Rep. 2025;15(1):44364. doi:10.1038/s41598-025-28091-6.
21. Kamboj RK, Singh M, Singh A, Bala A. Explainable artificial intelligence driven estimation of remaining useful life for lithium-ion battery. Ionics. 2025;31(11):11711–28. doi:10.1007/s11581-025-06707-1.
22. Kamboj RK, Singh M, Singh A, Bala A. An intelligent fault detection (IFD) system for lithium-ion battery using machine learning approach. Sci Rep. 2025;15(1):32190. doi:10.1038/s41598-025-17145-4.
23. Zhang N, Li J, Ma Y, Wu K. Lithium-ion batteries state of health estimation based on optimized TCN-GRU-WNN. Energy Rep. 2025;13(9):2502–15. doi:10.1016/j.egyr.2025.02.007.
24. Zequera RAG, Rassõlkin A, Vaimann T, Kallaste A. Kolmogorov-Arnold networks for algorithm design in battery energy storage system applications. Energy Rep. 2025;13:2664–77. doi:10.2139/ssrn.5022278.
25. Zhang Z, Zhang R, Liu X, Zhang C, Sun G, Zhou Y, et al. Advanced state-of-health estimation for lithium-ion batteries using multi-feature fusion and KAN-LSTM hybrid model. Batteries. 2024;10(12):433.
26. Akiba T, Sano S, Yanase T, Ohta T, Koyama M. Optuna: a next-generation hyperparameter optimization framework. In: Proceedings of the 25th ACM SIGKDD International Conference on Knowledge Discovery & Data Mining; 2019 Aug 4–8; Anchorage, AK, USA. p. 2623–31.
27. Arbaoui S, Samet A, Ayadi A, Mesbahi T, Boné R. Data-driven strategy for state of health prediction and anomaly detection in lithium-ion batteries. Energy AI. 2024;17(11):100413. doi:10.1016/j.egyai.2024.100413.
28. Salih A, Raisi-Estabragh Z, Galazzo IB, Radeva P, Petersen SE, Lekadir K, et al. A perspective on Explainable artificial intelligence methods: SHAP and LIME. Adv Intell Syst. 2024;7(1):2400304. doi:10.1002/aisy.202400304.
29. Wang B, Chen Z, Zhang P, Deng Y, Li B. The lithium-ion battery temperature field prediction model based on CNN-Bi-LSTM-AM. Sustainability. 2025;17(5):2125. doi:10.3390/su17052125.